A&A 486, 1009–1013 (2008)
DOI: 10.1051/0004-6361:20078976

Astronomy & Astrophysics

Comparison of SOHO UVCS and MLSO MK4 coronameter densities

K.-S. Lee[1], Y.-J. Moon[1], K.-S. Kim[1], J.-Y. Lee[1], K.-S. Cho[2], and G. S. Choe[1]

[1] Department of Astronomy and Space Science, Kyung Hee University, Yongin 446-701, Korea
e-mail: [moonyj;lksun]@khu.ac.kr
[2] Korea Astronomy and Space science Institute, Hwaam-dong, Yuseong-gu, Daejeon 305-348, Korea

Received 1 November 2007 / Accepted 11 April 2008

ABSTRACT

We have compared the density distributions of solar corona obtained by SOHO Ultraviolet Coronagraph Spectrometer (UVCS) and Mauna Loa Solar Observatory (MLSO) MK4 coronameter. This is the first attempt to compare the coronal densities estimated by the two instruments. In the spectral data of UVCS, we have selected two emission lines (O VI 1032 Å and 1037.6 Å), which have both radiative and collisional components. The coronal number density is determined from the ratio of these two components. The MK4 coronameter has a field of view ranging from 1.08 to 2.85 solar radii. The coronal density can be determined by inverting MLSO MK4 polarization maps. We find that the mean electron number density in a helmet streamer observed by MK4 on 2003 April 28 is fairly consistent with that observed by UVCS. For a coronal hole and an active region observed on 1999 October 19 and 24, the MK4 coronal densities are close to those from the UVCS within a factor of two; the former values are twice the latter at 1.7 solar radii and closer to the latter at higher altitudes. Our results demonstrate that MK4 polarization data can provide us with a coronal density distribution in a large field of view with a time cadence of about three minutes. We suggest that the MK4 data can be used to derive 2-D density distributions of coronal structures and further to estimate the heights of CME-associated type II shocks.

Key words. Sun: corona – Sun: UV radiation – methods: observational – techniques: spectroscopic

1. Introduction

The derivation of solar coronal density is very important in that it constrains the estimation of solar wind velocity, temperature and element abundances. Methods of determining the coronal electron density with different observations have been investigated by quite a few authors (van de Hulst 1950; Newkirk 1961; Noci et al. 1987; Akmal et al. 2001). Radio observation and extreme ultraviolet spectroscopy are powerful complementary diagnostic tools with which we can obtain such important information as coronal electron density and temperature of solar coronal plasma (Mancuso et al. 2003). In radio observations, for instance, we are able to derive the electron density by estimating the depth of the structure along the line of sight from the optical depth of free-free emission (Akmal et al. 2001). In UV spectral observations, some density sensitive lines (Keenan et al. 1995; Pinfield et al. 1998; Akmal et al. 2001) can be used with the CHIANTI atomic data base to derive the coronal density. The ratio of radiative and collisional components of the O VI doublet in UV spectra also gives density diagnostics (Noci et al. 1987; Parenti et al. 2000; Ko et al. 2006; Uzzo et al. 2006). On the other hand, white light observations can also provide the electron density distribution of the solar corona (Van de Hulst 1950). In white light observations, the electron density distribution is inferred from a polarization brightness map (van de Hulst 1950; Jackson et al. 1979; Hayes et al. 2001; Cho et al. 2007).

In this paper, we compare the electron densities obtained by two different methods using ultraviolet spectra and white light polarized brightness observations, respectively. In the first method, electron density is derived from the ratio of radiative and collisional components of the O VI 1032 Å and 1037.6 Å doublet as described in the previous paragraph. This method is often applied to coronal structures in streamers and in active regions. In the second method, we derive the coronal density distribution by inverting the polarized brightness (pB) map from the MLSO MK4 coronameter (van de Hulst 1950; Hayes et al. 2001; Cho et al. 2007). The UVCS measures the line intensity along the slit (1-D distribution) while the MK4 coronameter provides a two-dimensional polarization map. Mancuso et al. (2003) suggested that UVCS data should be used to infer the background pre-shock coronal density profiles. Cho et al. (2007) showed that white light observations of the MK4 coronameter can be used to infer the radial coronal density distribution near a helmet streamer that seems to be associated with the formation of coronal type II shocks.

The two methods give line of sight, averaged densities that are weighted very differently. Both tend to give densities near the plane of the sky because that is where the LOS passes closest to the Sun, so the density and dilution factor are largest. Nevertheless, they could be different if the density distribution is far from spherical or if the O VI concentration varies strongly. Comparison of the two methods tests the overall accuracy of both methods and gives an idea of the importance of the different weighting factors. The present study is the first attempt to compare the electron densities from both methods.

In this study we consider data for three different regions: (1) a helmet streamer; (2) the boundary between a coronal hole and an active region (hereafter *BCA*); and (3) an active region. We describe in detail the observations by the UVCS and MK4 coronameter in Sect. 2. In Sect. 3 we present the analysis method determining the coronal electron density in those regions. Then, we present the results of the density measurements from the two instruments and compare them. We also compare these results with the model by Newkirk (Newkirk 1961). In the last section, a brief summary and conclusion are given.

Table 1. Observational characteristics of three data sets.

Date	Structure	Slit position		Spatial res. (arcsec)		Temporal res. (s)		Time interval (UT)		Points
		Height ($R_\odot$)	PA (°)	UVCS	MK4	UVCS	MK4	Start	Finish	(Δt^2 < 1 min)
2003 April 28	Streamer	1.75	55	70	20	120	180	23:28	01:26	28
1999 October 19	Boundary[1]	1.46–3.5	270	21	20	180	180	17:30	18:34	20
1999 October 24	Active region	1.7–3.5	278	21	20	200	180	17:10	19:07	29

[1] Boundary consists of both open and closed field regions between the coronal hole and the active region.
[2] Observing time difference of the two instruments.

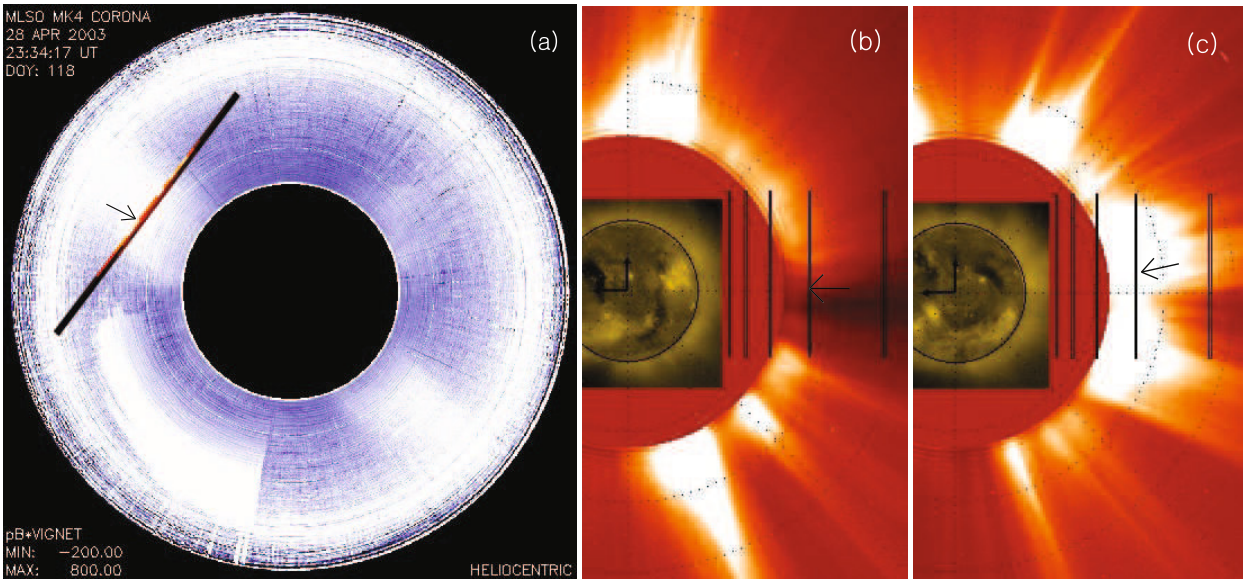

Fig. 1. UVCS slit positions projected on the plane of the sky. Black bars indicate the slit positions of UVCS. **a)** The UVCS slit superposed on the MK4 coronagraph image for the streamer on 28 April 2003. **b)** A composite image of the UVCS slits, the EIT image at 195 Å and the LASCO C2 image for the *BCA* on 19 October 1999. **c)** Composite image of the UVCS slits, the EIT image at 284 Å and the LASCO C2 image for the active region on 24 October 1999. Arrows indicate the slit positions where we measured the electron density.

2. Observations

In order to compare the electron densities from UVCS and MK4 for different coronal structures, we select three data sets: 2003 April 28, 1999 October 19, and 1999 October 24 (see Table 1). These sets are classified as the streamer, *BCA* and active region, respectively. For the comparison, we choose the data pairs (UVCS and MK4) whose observing time difference is within one minute and in which the O VI bright region in UVCS is located in the field of view of MK4. In Table 1, we describe the observational characteristics of each data set such as the slit positions of UVCS, spectral and temporal resolutions of UVCS and MK4 coronameter, time interval, number of data points, etc.

2.1. UVCS observation

The UVCS (Kohl et al. 1995) for the SOHO mission is designed for ultraviolet spectroscopy and visible light polarimetry of the extended solar corona with high spectral resolution. It measures the profiles of ultraviolet emission lines in the corona along a slit, which can be placed from 1.4 $R_\odot$ to as high as 12 $R_\odot$. It has two spectral channels: the O VI channel in the spectral range of 945−1123 Å and the Lyα channel in the range of 1160−1350 Å. Our observations were obtained with the O VI channel that contains the O VI doublet 1032 Å and 1037.6 Å.

Figure 1a shows the UVCS slit and the MK4 observation of the 2003 April 28 data. Figures 1b and 1c are composite images produced by combining images from the EUV Imaging Telescope (EIT) at 195 and 284 Å for the lower corona, the UVCS slits and the Large Angle and Spectrometric Coronagraph (LASCO) C2 observations on 1999 October 19 and 24, respectively.

For the 2003 April 28 data, UVCS observed a streamer which had a helmet structure with good radial and latitudinal extent, as described by Uzzo et al. (2006). A typical exposure time of UVCS is 120 s. We have selected 28 data sets for 2 h, which were simultaneously observed by MK4. The slit of the UVCS is located with a position angle of 55° at 1.75 $R_\odot$, as shown in Fig. 1a. The spatial resolution of the data is 70″ with a spatial binning of 10 pixels. Its spectral resolution is 0.36 Å for primary wavelengths with a spectral binning of 2 pixels with 98 μm slit width.

The UVCS slits for observation of the *BCA* and the active region on 1999 October 19 and 24 were respectively located at position angles 270° and 278°. The UVCS observed the corona with the slit positioned at a height of 1.46, 1.7, 2.05, 2.6, and 3.5 $R_\odot$.The slit on the highest solar height of 3.5 $R_\odot$ is not considered in this analysis because the MK4 coronameter covers from 1.08 $R_\odot$ to 2.85 $R_\odot$. The data were obtained with a spatial binning of 3 pixels, 21″. The *BCA* was observed with a spectral binning of 3 pixels, while the active region was observed with a spectral binning of 2 pixels. Figure 1b shows the equatorial coronal hole at the west limb. The brightness of the O VI emission increased as the active region moved toward the limb as shown in Fig. 1c.

For the wavelength and radiometric calibration of UVCS data, we used DAS40 (Data Analysis Software). The density diagnostic using these data is described in Sect. 3.1.

2.2. MK4 observation

The MK4 coronameter (Elmore et al. 2003) provides white light polarized brightness (pB) maps in the wavelength range from 700 to 950 nm with a 3 min cadence and an angular resolution of about 20″. It has a field of view from 1.08 to 2.85 $R_\odot$, over which a two dimensional density distribution as a function of radial height and position angle can be obtained from the MK4 polarization brightness map. To estimate the coronal density distribution from the MK4 polarization maps, we used a standard routine (pb_inverter.pro) in the SolarSoft package. The inversion method is described in Sect. 3.2.

3. Density comparison

3.1. Density diagnostics from UVCS

To estimate the electron density of coronal structures, we use the O VI doublet, which is among the brightest lines in UVCS spectra, even though its lines are not particularly density sensitive. We infer the electron density from the ratio of radiative and collisional components of the O VI doublet (Parenti et al. 2000; Antonucci et al. 2005; Ko et al. 2006; Uzzo et al. 2006). In a region with negligible outflow, the two components of the O VI at 1032 Å and 1037 Å can be derived from the observed total intensity, the ratio of collisional components of the two lines and the ratio of radiative components of the two lines (Raymond et al. 1997);

$$I_{\rm total} = I_{\rm rad} + I_{\rm col}, \tag{1}$$

$$\frac{I_{\rm col}(1032)}{I_{\rm col}(1037)} = 2, \qquad \frac{I_{\rm rad}(1032)}{I_{\rm rad}(1037)} = 4. \tag{2}$$

In such a region, collisional and radiative components depend on $N_{\rm e}^2$ and $N_{\rm e}$, respectively. According to Noci et al. (1987), we determine $N_{\rm e}$ using the following relation:

$$\frac{I_{\rm rad}}{I_{\rm col}} = 5.75\times10^2\,\frac{\lambda^2\exp(E/kT_{\rm e})\sqrt{T_{\rm e}}I_{1032,\,\rm disk}}{\overline{g}N_{\rm e}(\Delta\lambda_{\rm cor}^2+\Delta\lambda_{\rm ex}^2)^{1/2}}\frac{R_\odot^2}{r^2}h(r), \tag{3}$$

where $\lambda = 1031.9$ Å, the transition energy between the levels responsible for O VI λ 1032 line $E = 1.9251\times10^{-11}$ erg, k the Boltzmann constant, $\overline{g} = 1.13$ the effective Gaunt factor, and $h(r) = 2[1-(1-R_\odot^2/r^2)^{0.5}]r^2/R_\odot^2$. For other parameters ($\Delta\lambda_{\rm cor}$, $\Delta\lambda_{\rm ex}$, and $I_{1032,\,\rm disk}$), we refer to the values by Uzzo et al. (2006) and Ko et al. (2006) for each observation. The wavelength $\Delta\lambda_{\rm ex}$ is the e-folding half-width of the exciting line from the lower atmosphere (0.10 Å for the streamer in 2003 and 0.121 Å for the BCA and the active region in 1999) and $\Delta\lambda_{\rm cor}$ is the e-folding half-width of the coronal absorption profile (0.145 Å for the streamer and 0.194 Å for the BCA and the active region). $I_{1032,\,\rm disk}$ is the line intensity of λ 1032 integrated over the disk. It is determined from each observation with the value of the disk intensities from Vernazza & Reeves. (1978). The electron temperature, $T_{\rm e}$, is an independent parameter to be obtained by a separate procedure. We used constant coronal temperatures (1.74 MK for the streamer, 1.65 MK for BCA and 1.7 MK for the active region) from Uzzo et al. (2006) and Ko et al. (2006), who estimated them using the temperature sensitive lines Fe X, Fe XII, Fe XIII.

Table 2. Electron density at 1.7 $R_\odot$ for three coronal structures obtained from UVCS and MK4 coronameter.

Date	$N_{\rm e}$ (10^6 cm^{-3})	
	UVCS	MK4
2003 April 28	17.8 ± 4.8	18.7 ± 1.7
1999 October 19	5.45 ± 1.56	9.93 ± 0.52
1999 October 24	14.1 ± 2.0	29.8 ± 1.2

Using the above equations and parameters, we can derive the values of $I_{\rm rad}/I_{\rm col}$ for the λ 1032 line and then determine $N_{\rm e}$. We have estimated the coronal density in three different structures (Table 1): the streamer, the BCA, and the active region. For the streamer on 2003 April 28, the density at 1.75 $R_\odot$ is estimated to be 1.78×10^7cm^{-3}, which is in good agreement with that of Uzzo et al. (2006). The electron densities in the BCA and the active region are obtained at different heights. In both structures, the density decreases with heliocentric distance, and the density in the active region is higher than the value in the BCA at all heights. The electron densities at 1.7 $R_\odot$ are given in Table 2.

3.2. Density determination from the MK4 coronameter

Now we infer the electron density from the polarization brightness obtained from the MK4 coronameter using an inversion method. The measurement of pB is defined as the difference between the tangential and radial polarization components of the K corona, the F corona and the scattered light (Hayes et al. 2001) as

$$pB = B_{\rm t} - B_{\rm r} = K_{\rm t} - K_{\rm r} + F_{\rm t} - F_{\rm r} + S_{\rm t} - S_{\rm r}. \tag{4}$$

The K coronal component arises from the Thompson scattering by free electrons, and the F coronal component from scattering of photospheric light by dust in the interplanetary medium. In general, K and F coronal contributions are mixed together. To evaluate the coronal electron density, we have to subtract the F coronal component from pB. The otherwise scattered light, S, can be neglected.

The routine that we used to derive the electron density was originally developed using an inversion method by van de Hulst (1950). We used an improved inversion method by Hayes et al. (2001), who eliminated the F corona using a empirical model from the LASCO and the Polarimetric Instrument for Solar Eclipse (POISE) observations. In the method, three assumptions are made as follows:

1. the K corona is completely polarized while the F corona is unpolarized;
2. the coronal density is axisymmetric;
3. the electron density along the radial direction can be expressed in a polynomial form.

We can separate the K and F corona by a method based on assumption (1). pB records only K coronal signals since unpolarized signals of the F corona do not contribute to pB

$$pB = K_{\rm t}(x) - K_{\rm r}(x) = C\int_x^\infty N(r)\,[A(r)-B(r)]\frac{x^2{\rm d}r}{r\sqrt{(r^2-x^2)}}, \tag{5}$$

where C is a unit conversion factor (3.44×10^{-6}cm^{-3}), N is the electron density, A and B are geometric factors, x is the impact parameter, and r is the radial height from solar center (van de Hulst 1950; Hayes et al. 2001). The field of view of the MK4 coronameter covers 1.2 $R_\odot$ to 2.8 $R_\odot$.

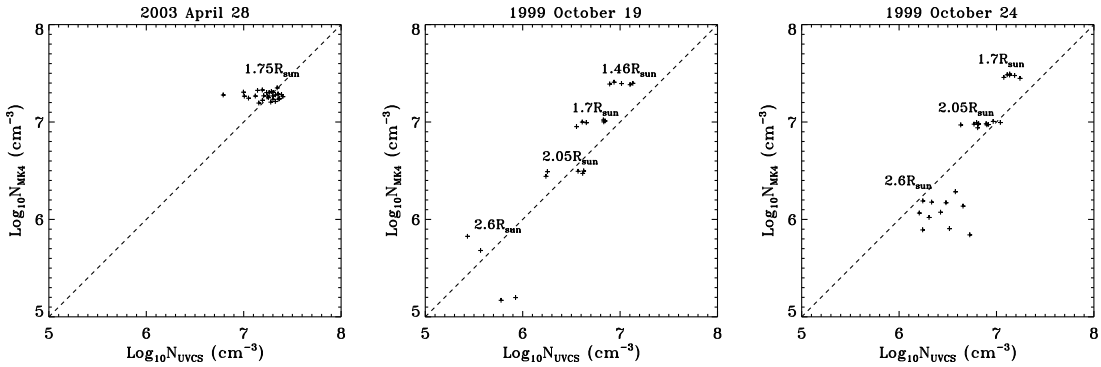

Fig. 2. Comparison of the coronal densities of three structures obtained from UVCS and MK4 coronameter observations. **a)** 2003 April 28. **b)** 1999 October 19. **c)** 1999 October 24. The abscissa represents the UVCS density and the ordinate the MK4 density, both on a logarithmic scale. The dashed line indicates equality of the two densities.

The electron densities obtained by this method from the two dimensional pB maps for three coronal structures are listed in Table 2. The derived values are $18.7\pm1.7\times10^6$ cm^{-3} at 1.75 $R_\odot$ in the streamer, and $9.93\pm0.52\times10^6$ cm^{-3} and $29.8\pm1.2\times10^6$ cm^{-3} at 1.7 $R_\odot$ in the *BCA* and the active region, respectively.

3.3. Comparison of the two densities

In the previous subsections, we derived the coronal electron densities of three structures from two different data sets: the SOHO UVCS and the MLSO MK4 coronameter. Figure 2 shows the densities from the two instruments for those structures. We find that the coronal densities from the two instruments are fairly consistent with each other although the consistency depends on region and height.

For the helmet streamer on 2003 April 28 (Fig. 2a), the UVCS observation was made only at 1.75 $R_\odot$ for about two hours. The mean densities from each instrument are in good agreement with each other (see Table 2). The MK4 density is about 5% higher than the UVCS density on average. For the second and third structures on 1999 October 19 and 24 (Figs. 2b and c), the MK4 coronal densities are about twice as high as the UVCS densities around 1.7 $R_\odot$. The difference between the mean densities becomes small with increasing altitude, but the individual values are more dispersed. Particularly, the MK4 densities at 2.59 $R_\odot$ are rather widely spread, which may be caused by the discontinuity of the inversion method at 2.5 $R_\odot$ due to the F corona contribution (Hayes et al. 2001).

One may ask why the MK4 densities are higher than the UVCS ones. A cause of such a difference may be the fact that they are differently weighted averages. The MK4 density is weighted by a dilution factor, while the UVCS density is weighted also by the O VI density,

$$pB \propto \int n_e W \mathrm{d}r, \tag{6}$$

$$\frac{I_{\rm rad}}{I_{\rm col}} \propto \frac{\int n_{\rm ovi} W \mathrm{d}r}{\int n_e n_{\rm ovi} q \mathrm{d}r}. \tag{7}$$

Here, q is the collisional excitation rate, and W is the dilution factor of the disk radiation which is expressed as, $W = \frac{1}{2}[1 - \sqrt{1-(\frac{r_*}{r})^2}]$, where r_* is the radius of the radiating surface and r denotes the position of the observer. In Eq. (3), the density determination method using UVCS is indeed independent of the oxygen abundance and ionic fraction, because these two quantities enter the ratio of radiative to collisional contributions in the same manner and cancel out. Therefore, we would expect to find the same density using either the O VI ratio or the polarized brightness. In Eqs. (6) and (7), however, the density derived from pB is weighted by the dilution to the place where the line of sight passes closest to the Sun while the density derived from the O VI ratio is weighted toward regions where the O VI concentration is high. Therefore, if plasma is concentrated in a streamer near the plane of the sky, rather than being in a spherical distribution, the two could give somewhat different answers depending on the oxygen abundance and ionization state (Raymond, private communication). Moreover Raymond et al. (1997) described the systematic difference in the abundance derived for the collisional and radiative contributions from the quiescent streamer center, leg, and active regions. They found an anti-correlation between density and abundance. We speculate that the depletion of O in the streamer core (Raymond et al. 1997) would tend towards the observed sense of the difference between MK4 and UVCS if the density is highest in the streamer core and drops off toward the edges, where a higher O abundance is often observed.

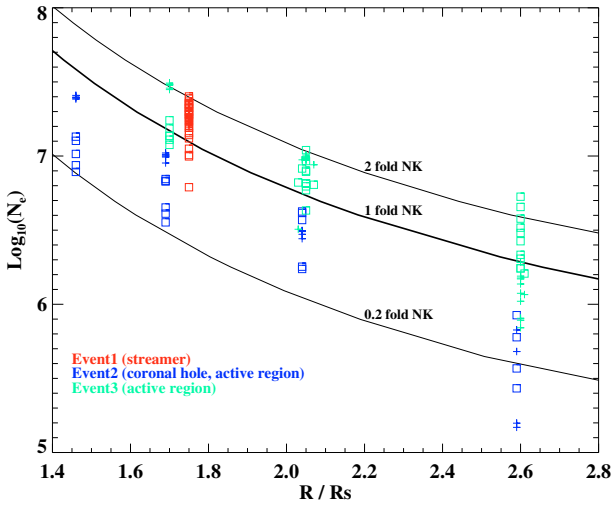

Fig. 3. Comparison of the observed densities with the Newkirk models. The solid lines represent 0.2, one and two-fold Newkirk models. The crosses indicate the N_e from the MK4 coronameter, and the squares denote the N_e from the UVCS.

We compared the observed densities with the conical active region model by Newkirk (1961) in Fig. 3. This model has been often employed to derive coronal shock speeds from type II radio burst observations. As shown in the figure, the derived densities

for the streamer on 2003 April 28 (red) and the active region on 1999 October 24 (green) are placed between the one-fold and two-fold Newkirk models, and the densities for the *BCA* on 1999 October 19 (blue) are located between the one-fold and 0.2 fold Newkirk models.

4. Summary and conclusion

In this paper, we compared the coronal electron densities obtained from the UVCS and from the MK4 coronameter. We derived the electron densities at 1.4 $R_\odot$−2.6 $R_\odot$ in three different coronal structures. The main results of our study can be summarized as follows. First, for a helmet streamer on 2003 April 28, the mean number density derived from the MK4 data is in good agreement with that derived from the UVCS data. Second, for the coronal hole and the active region observed on 1999 October 19 and 24, the MK4 coronal densities are close to those from the UVCS within a factor of two; the former are twice as high as the latter at 1.7 solar radii and move closer to the latter at higher altitude. Third, a comparison between the observed densities and the Newkirk models shows that the derived densities for the streamer on 2003 April 28 and the active region on 1999 October 24 are placed between the one-fold and two-fold Newkirk models, and the densities for the *BCA* on 1999 October 19 are located between the one-fold and 0.2 fold Newkirk models.

Our results demonstrate that MK4 polarization data can provide us with the 2-D coronal density distribution of a large field of view with about a three minute temporal cadence. Recently, Cho et al. (2007) derived type II shock heights using the MK4 density distribution instead of the Newkirk coronal density model that has been widely adopted. Bemporad et al. (2007) also used the coronal density distribution from MK4 coronameter to derive a CME density distribution on an occasion for which UVCS data were not available. Since our study confirms the validity of deriving coronal density from MK4 data, the MK4 density distribution with three minute time cadence can be utilized for diverse scientific purposes, as shown in the above examples.

Acknowledgements. We appreicate the referee's constructive comments. We are very thankful to Dr. J. C. Raymond and Dr. Y.-K. Ko for their very constructive comments. This work has been supported by the Korea Research Foundation grant (KRF-2005-070-C00059 and ABRL-R14-2002-043-01001-0), the second stage BK21 project of Korean Research Foundation, the KASI basic research fund, and the second stage Kyoung Hee University graduate research scholarship in 2007. SOHO is a project of international cooperation between ESA and NASA.

References

Akmal, A., Raymond, J. C., Vourlidas, A., et al. 2001, ApJ, 553, 922
Antonucci, E., Abbo, L., & Dodero, M. A. 2005, A&A, 435, 699
Bemporad, A., Raymond, J. C., Poletto, G., & Romoli, M. 2007, ApJ, 655, 576
Chapman, S. 1957, Smithsonian Contrib. Astrophys., 2, 1
Cho, K.-S., Lee, J., Moon, Y.-J., et al. 2006, A&A, 461, 1121
Elmore, D. F., Burkepile, J. T., Darnell, J. A., Lecinski, A. R., & Stanger, A. L. 2003, Proc. SPIE, 4843
Hayes, A. P., Vourlidas, A., & Howard, R. A. 2001, ApJ, 548, 1081
Jackson, B. V., Sheridan, K. V., & Dulk, G. A. 1979, Proc. Astron. Soc. Aust., 3, 387
Keenan, F. P., Brekke, P., Byrne, P. B., & Greer, C. J. 1995, MNRAS, 276, 915
Ko, Y.-K., Raymond, J. C., Zurbuchen, T. H., et al. 2006, ApJ, 646, 1275
Kohl, J. L., Esser, R., Gardner, L. D., et al. 1995, Sol. Phys., 162, 313
Mancuso, S., Raymond, J. C., Kohl, J., Ko, Y.-K., & Wu, R. 2003, A&A, 400, 347
Newkirk, G., Jr. 1961, ApJ, 133, 983
Noci, G., Kohl, J. L., & Withbroe, G. L. 1987, ApJ, 315, 706
Parenti, S., Bromage, B. J. I., Poletto, G., et al. 2000, A&A, 363, 800
Pinfield, D. J., Mathioudakis, M., Keenan, F. P., Phillips, K. J. H., & Curdt, W. 1998, A&A, 340, L15
Raymond, J. C., Kohl, J. L., Noci, G., et al. 1997, Sol. Phys., 175, 645
Uzzo, M., Strachan, L., Vourlidas, A., Ko, Y.-K., & Raymond, J. C. 2006, ApJ, 645, 720
van de Hulst, H. C. 1950, Bull. Astron. Inst. Netherlands, 11, 135
Vernazza, J. E., & Reeves, E. M. 1978, ApJS, 37, 485